Development 134, 3723-3732 (2007) doi:10.1242/dev.008599

Long form of latent TGF-β binding protein 1 (Ltbp1L) is essential for cardiac outflow tract septation and remodeling

Vesna Todorovic[1,*], David Frendewey[2], David E. Gutstein[1,3], Yan Chen[1], Laina Freyer[1,†], Erin Finnegan[1], Fangyu Liu[3], Andrew Murphy[2], David Valenzuela[2], George Yancopoulos[2] and Daniel B. Rifkin[1,3]

Latent TGF-β binding protein 1 (LTBP1) is a member of the LTBP/fibrillin family of extracellular proteins. Due to the usage of different promoters, LTBP1 exists in two major forms, long (L) and short (S), each expressed in a temporally and spatially unique fashion. Both LTBP1 molecules covalently interact with latent TGF-β and regulate its function, presumably via interaction with the extracellular matrix (ECM). To explore the in vivo role of Ltbp1 in mouse development, at the time when only the L isoform is expressed, we mutated the *Ltbp1L* locus by gene targeting. *Ltbp1L*-null animals die shortly after birth from defects in heart development, consisting of the improper septation of the cardiac outflow tract (OFT) and remodeling of the associated vessels. These cardiac anomalies present as persistent truncus arteriosus (PTA) and interrupted aortic arch (IAA), which are associated with the faulty function of cardiac neural crest cells (CNCCs). The lack of Ltbp1L in the ECM of the septating OFT and associated vessels results in altered gene expression and function of CNCCs and decreased Tgf-β activity in the OFT. This phenotype reveals a crucial role for Ltbp1L and matrix as extracellular regulators of Tgf-β activity in heart organogenesis.

KEY WORDS: LTBP1, TGF-β, ECM, OFT septation, Mouse

INTRODUCTION

The four latent TGF-β binding proteins (LTBP1-4) belong to the LTBP/fibrillin family of large extracellular glycoproteins (Todorovic et al., 2005). LTBP1, LTBP3 and LTBP4 form a subgroup within the family, because they covalently interact with latent TGF-β. Latent TGF-β is a dimer of the mature cytokine non-covalently bound to its propeptide, the latency associated protein (LAP). This complex is referred to as the small latent complex (SLC), whereas the tri-molecular complex composed of an LTBP and the SLC is dubbed the large latent complex (LLC). Numerous in vitro experiments have indicated the importance of LTBPs as regulators of TGF-β function: LTBPs facilitate the secretion of latent TGF-β, direct its localization in the extracellular matrix (ECM) and regulate the activation of the cytokine. Ablation of the *Ltbp3* gene and attenuation of *Ltbp4* expression (Dabovic et al., 2002; Sterner-Kock et al., 2002) both result in developmental defects associated with reduced Tgf-β activity, further demonstrating that Ltbp3 and Ltbp4 modulate extracellular Tgf-β levels in a specific and non-redundant manner.

Multiple in vitro studies have indicated that LTBP1 also plays an important role in the regulation of TGF-β bioavailability. For example, addition of an antibody to LTBP1 blocked latent TGF-β activation in co-cultures of endothelial and smooth muscle cells (SMCs) (Flaumenhaft et al., 1993). Similarly, antibodies to LTBP1 blocked epithelio-mesenchymal transition (EMT) in atrio-ventricular (AV) cushion explants (Nakajima et al., 1997) and prevented embryonic stem cell differentiation into endothelial cells (Gualandris et al., 2000). Mouse embryonic fibroblasts (MEFs) lacking dioxin receptor (AhR) display increased apoptosis correlated with a higher production of Ltbp1L and augmented TGF-β1 activity (Gomez-Duran et al., 2006). A decrease in Ltbp1L restored the normal levels of Tgf-β1 in $AhR^{-/-}$ MEFs, suggesting that Ltbp1L contributes to maintaining active Tgf-β1 levels (Gomez-Duran et al., 2006). Thus, all the aforementioned reports indicate a role for LTBP1 in latent TGF-β activation. Indeed, we have shown that LTBP1 is essential for αvβ6-mediated TGF-β1 activation and that other LTBPs cannot substitute for LTBP1 (Annes et al., 2004).

LTBP1 exists in two major forms – short (S) and long (L) (Fig. 1A) – which are transcribed from independent promoters (Koski et al., 1999). Ltbp1L is the only form expressed during embryonic development, whereas the S form first appears in the late fetal period to become the prevalent form in the adult (Weiskirchen et al., 2003). Both forms of LTBP1 bind latent TGF-β; however, the L form interacts with the ECM more efficiently (Olofsson et al., 1995).

Perinatal lethality in mice lacking Tgf-β2 and Tgf-β3 suggests an indispensable role for these isoforms in organogenesis. Given that Ltbp1L, but not Ltbp1S, is expressed in mouse embryos, we were interested in exploring the in vivo function of Ltbp1L. We have targeted the murine *Ltbp1L* gene, generating mice with congenital heart defects consisting of improper septation of the cardiac outflow tract (OFT) and aberrant maturation of the associated vasculature. These cardiac abnormalities manifest as persistent truncus arteriosus (PTA) and interrupted aortic arch (IAA), both of which have been previously associated with malfunction of a specific embryonic cell population, termed cardiac neural crest cells (CNCCs).

CNCCs originate from the dorsal neural tube between the mid-otic placode and the third somite (Jiang et al., 2000). At embryonic day (E)9.5 in mice, CNCCs delaminate from the rhombencephalon and migrate latero-ventrally along pharyngeal arch arteries (PAAs) 3, 4 and 6, towards the cardiac tissue. A subset of CNCCs remains within the pharyngeal arches 3, 4 and 6, in which they participate in supporting and remodeling of PAAs. Other CNCCs invade the cardiac OFT, where they proliferate, condense and form the aortico-pulmonary (AP) septum, a structure crucial for division of the OFT into aortic and pulmonary vessels (Jiang et al., 2000; Kirby and Waldo, 1995).

[1]Cell Biology Department, NYU School of Medicine, New York, NY 10016, USA. [2]Regeneron Pharmaceuticals, Tarrytown, NY 10591, USA. [3]Department of Medicine, NYU School of Medicine, New York, NY 10016, USA.

*Author for correspondence (e-mail: todorv01@med.nyu.edu)
[†]Present address: Albert Einstein College of Medicine, Department of Molecular Genetics, Bronx, NY 10461, USA

Accepted 26 July 2007

Numerous reports have emphasized the role of TGF-β in the proper function of CNCCs. TGF-β proteins signal through a heteromeric complex of type I and type II receptors (Massague et al., 2000). Deletion of either Tgf-β type I or type II receptor specifically from the neural crest results in PTA and IAA (Choudhary et al., 2006; Wang et al., 2006; Wurdak et al., 2005), demonstrating that functional Tgf-β signaling in CNCCs is essential for normal OFT septation and remodeling.

Here, we describe *Ltbp1L*$^{-/-}$ animals with congenital heart defects, comprising PTA and IAA. The absence of Ltbp1L in the OFT and pharyngeal ECM resulted in decreased Tgf-β activity, affected the gene expression of CNCCs and caused their malfunction. Our results emphasize the importance of Ltbp1L and its potential ECM interactions as a crucial extracellular regulator of Tgf-β bioavailability during heart development.

MATERIALS AND METHODS

Generation of *Ltbp1L*$^{-/-}$ mice

Two null alleles (designated as A and B) of the mouse *Ltbp1L* gene were constructed (see Results). To create the *Ltbp1L*-deletion alleles we used VelociGene methods (Valenzuela et al., 2003) to modify a bacterial artificial chromosome (BAC) clone carrying the mouse *Ltbp1L* gene by replacement of the deleted sequence with the expression-selection cassette by homologous recombination (Muyrers et al., 1999). The targeting vectors for each allele were made by linearization of the modified BAC, producing homology arms of ~150 kb and 30 kb flanking the deletion. After electroporation of the targeting vectors into SvEv129/C57Bl6/F1-derived hybrid embryonic stem (ES) cells (Valenzuela et al., 2003), clones that scored for loss of one of the *Ltbp1L* alleles were identified by LONA assay.

Northern blot analysis

Total RNA was isolated from wild-type and *Ltbp1L* knockout (KO) E14.5 embryos and E17.5 immortalized MEFs, using Trizol Reagent (Invitrogen) and following the manufacturer's protocol. RNA (20 μg) of each genotype was loaded on 1% agarose gel. The gel was stained with ethidium bromide and the amount of 18S RNA used for internal standardization. Northern blotting was performed as described at http://www.fhcrc.org/science/labs/breeden/Methods/Northern_Blot.html. [α-^{32}P]-dCTP-labeled mouse *Ltbp1L* cDNA (Noguera et al., 2003) was used as a probe.

Immunoblotting

Protein extracts from E14.5 wild-type and KO hearts were made by homogenizing each frozen heart in 40 μl of ice-cold RIPA buffer (1% Na-deoxycolate; 50 mM Tris pH 7.5; 150 mM NaCl; 1% Nonidet P40) with protease inhibitors (Roche). The protein extracts were separated on 4-12% non-reducing SDS gels and blotted with Ab39 (Annes et al., 2004).

X-gal staining

E9.5-E12.5 embryos were stained with X-gal as described (Deckelbaum et al., 2006). Stained embryos were post-fixed in 4% PFA in PBS ON/+4°C and processed for paraffin embedding.

In situ hybridization and probes

Anti-sense ribo-probes for *Crabp1* (construct from A. Baldini, Baylor College of Medicine, TX), plexin A2 (construct from J. Epstein, UPenn, PA), *FoxC1* (construct from B. Hogan, Duke University, NC) and *Ctgf* (construct from H. Heuer, Leibniz-Institut, Germany) were digoxigenin labeled using adequate primers and RNA polymerase (Roche). In situ hybridization on paraffin sections was performed as described at http://www.med.upenn.edu/mcrc/histology_core/nrinsitu.shtml. Whole-mount in situ hybridization was performed as described (Deckelbaum et al., 2006).

Quantification of mesenchymal cells in the OFT

The number of mesenchymal cells in the OFT of control and mutant E11.5 littermates was determined in transverse sections every 40 μm. Three pairs of control and mutant E11.5 littermates were used and the average numbers of this quantification were plotted. Quantification of phospho-histone 3-positive cells was performed identically.

Immunohistochemistry

Antigen retrieval from paraffin sections was performed in DakoCytomation Target Retrieval Solution for 20 minutes at 95°C; or in Na-citrate pH 6, heated for 2 minutes in a microwave oven (phospho-Smad2). The following primary antibodies were used: rabbit polyclonal phospho-histone 3, Cell Signaling; monoclonal α-smooth muscle actin 1A4, Sigma; rabbit monoclonal cleaved caspase 3, Cell Signaling; rabbit polyclonal phospho-Smad2, Chemicon; and TGF-β2, Santa Cruz.

India ink injections

Injections of India ink in E10.5-E11.5 embryonic hearts were performed as described (Kaartinen et al., 2004).

Detecting CNCCs distribution in the OFT of *Ltbp1L* KO mice

To detect the distribution of neural crest-derived cells in the OFT of *Ltbp1L*$^{-/-}$ mice, the *EYFP-Cre* reporter strain (Srinivas et al., 2001) (provided by F. Costantini, Columbia University, NY) was crossed with *Wnt1-Cre* transgenic line (Jiang et al., 2000) (obtained from H. Sucov, USC, CA). Control and *Ltbp1L*$^{-/-}$ embryos expressing the EYFP reporter construct and the *Wnt1-Cre* transgene were sectioned, counter-stained with propidium-iodide and imaged by fluorescence microscopy at E10.5-E11.5.

Semi-quantitative and quantitative real-time RT-PCR analysis

RNA was extracted from three pairs of E11.5 control and KO hearts using the RNeasy Protect Mini kit (Qiagen) with DNase treatment included. Reverse transcription (RT) was performed using 50 ng of RNA and the Sensiscript Reverse Transcriptase (Qiagen). The resulting cDNA was used for semi-quantitative and quantitative real-time RT-PCR (Q-RT-PCR) analysis. Primers used in semi-quantitative PCRs (all shown 5′-3′): β-actinF, ATCTGGCACCACACCTTCTACAATGAGCTGCG; β-actinR, CGTCATACTCCTGCTTGCTGATCCACATCTGC; CtgfF, AAGAC-ACATTTGGCCCAGAC; CtgfR, TTACGCCATGTCTCCGTACA. PCR conditions: β-actin, (94°C/1′; 58°C/45″; 72°C/1′)×25; Ctgf, (94°C/1′; 60°C/45″; 72°C/1′)×35. Q-RT-PCRs were performed using specific primers in the presence of SYBR Green dye (Molecular Probes, Eugene, OR) on an iCycler Thermal Cycler (Bio-Rad). Each target transcript expression was quantified by comparing the threshold cycle (C_T) with that of hypoxanthine guanine phosphoribosyl transferase by using the comparative C_T method. Primers used: HPRT sense CTGGTGAAAAGGACCTCTCG, antisense CAAGGGCATATCCAACAACA; Tgf-β1 sense ACCCTGCCCCTAT-ATTTGGA, antisense TGGTTGTAGAGGGCAAGGAC; Tgf-β2 sense GAACCCAAAGGGTACAATGC, antisense TGGTGTTGTACAGGCT-GAGG; Tgf-β3 sense TATGCCAACTTCTGCTCAGG, antisense CTCT-GGGTTCAGGGTGTTGT; Ltbp3 sense GGTATGCGAGTGTCCTGGAG, antisense CAGTTCTCGGCACTCATCAA; c-Myc (Myc) sense GCTG-GAGATGATGACCGAGT, antisense AACCGCTCCACATACAGTCC.

RESULTS

Generation of *Ltbp1L*-null mice

We used VelociGene technology (Valenzuela et al., 2003) to create two *Ltbp1L* deletion alleles, designated as A and B (Fig. 1B). For the A allele, we made a 666 bp deletion including 457 bp of the 3′ portion of exon 1 and 209 bp of the downstream intron; whereas, for the B allele, we made a 7.8 kb deletion from the 165th codon of the *Ltbp1L* coding sequence in exon 2 through the remainder of exon 2 and into the downstream intron. The deleted sequences were replaced with an expression cassette comprising a β-galactosidase coding sequence (*lacZ*) fused in-frame with the upstream coding sequence of *Ltbp1L*, followed by a polyadenylation signal and an antibiotic selection cassette flanked by *loxP* sites. The targeting of embryonic stem (ES) cells and the germline transmission were confirmed by a quantitative reverse transcription PCR (Q-RT-PCR) assay that scored for the loss of one of the native *Ltbp1L* alleles (data not shown). The *neo*^{R} cassette was removed by crossing line A and B mice with mice expressing Cre recombinase in the germ cell

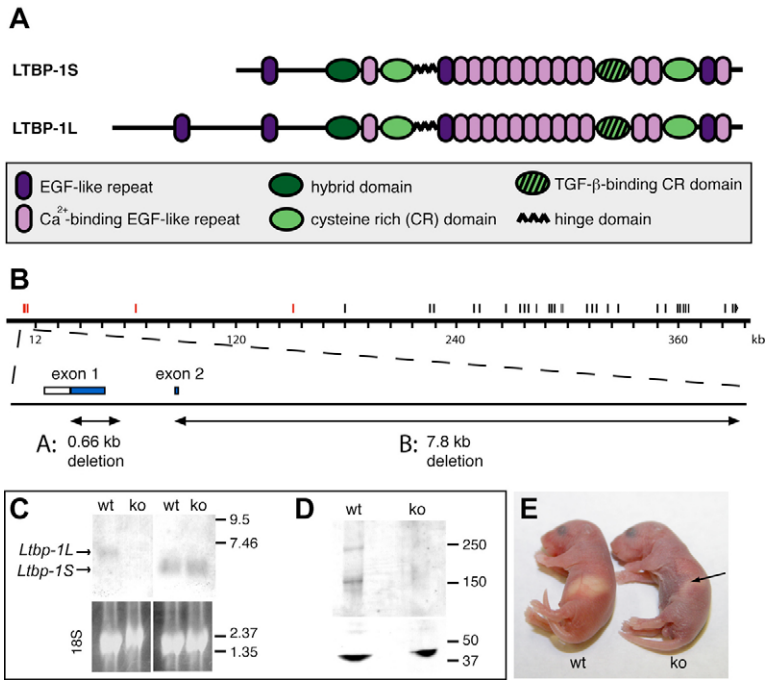

Fig. 1. Targeted inactivation of the *Ltbp1L* gene. (**A**) Schematic representation of the Ltbp1 short (S) and long (L) forms. (**B**) Targeting of the *Ltbp1L* locus. The *Ltbp1L* gene is composed of 34 exons (represented as vertical bars above the gene). Four exons specific for *Ltbp1L*, and not for *Ltbp1S*, are presented as red bars. Two null alleles, designated A and B, were generated. Deletion 'A' encompasses 457 bp of exon 1 and a portion of intron 1. Deletion 'B' is 7.8 kb long and includes most of exon 2 and a portion of intron 2. (**C**,**D**) Validation of *Ltbp1L* gene targeting. (C) Upper panels: northern blot with E14.5 wild-type and knockout (KO) RNA (left) and wild-type and KO RNA isolated from immortalized E17.5 MEFs (right), hybridized to a [^{32}P]-labeled *Ltbp1L* cDNA. Lower panels: RNA loading control. (D) Western blots with total-protein extracts isolated from wild-type and KO E14.5 hearts incubated with an Ltbp1 antibody (upper panels) and a β-actin antibody (lower panels). (**E**) Newborn control and *Ltbp1L*$^{-/-}$ mice. *Ltbp1L*$^{-/-}$ neonates are cyanotic and unable to suckle (arrow illustrates the lack of milk in the stomach).

lineage. A and B lines, with or without the *neo*^{R} cassette, showed the same phenotype; hence, both lines were used interchangeably with no differences observed.

Ltbp1L mRNA and protein are not detectable in *Ltbp1L*$^{-/-}$ mice

We screened total RNA isolated from E14.5 *Ltbp1L*$^{-/-}$ and wild-type embryos for *Ltbp1L*-specifc mRNA by northern blotting (Fig. 1C, left). A [^{32}P]-labeled full-length *Ltbp1L* cDNA was used as a probe, which visualized *Ltbp1L*- but not *Ltbp1S*-specific mRNA in our control sample. This result is in agreement with the description of *Ltbp1* embryonic expression, in which *Ltbp1S*-specific mRNA is first detected at around E17.5 (Weiskirchen et al., 2003). We did not detect any *Ltbp1*-specific mRNA in our knockout (KO) sample (Fig. 1C, left). However, we could detect *Ltbp1S* mRNA in immortalized wild-type and KO E17.5 fibroblasts (Fig. 1C, right), indicating that only *Ltbp1L* but not *Ltbp1S* expression is attenuated in *Ltbp1L*$^{-/-}$ mice. Western blot analysis of protein extracts from E14.5 wild-type and KO hearts revealed bands at the expected positions of the full-length (~240 kDa) and truncated (~170 kDa) forms of Ltbp1L in wild-type but not KO samples (Fig. 1D), confirming the ablation of the *Ltbp1L* gene.

Newborn *Ltbp1L*-null mice die from PTA and IAA

At birth, mice heterozygous for the *Ltbp1L* mutation were grossly indistinguishable from their wild-type littermates. However, *Ltbp1L*$^{-/-}$ newborns were cyanotic (Fig. 1E) and died just after birth. Only 55% (51 out of the expected 92) of *Ltbp1L* mutants (both lines A and B) were recovered at birth, suggesting embryonic lethality. The distribution of the wild-type, heterozygous and null embryos from heterozygous crosses was Mendelian until E14.5, when the percentage of mutant embryos decreased by 40% (14 out of the expected 30).

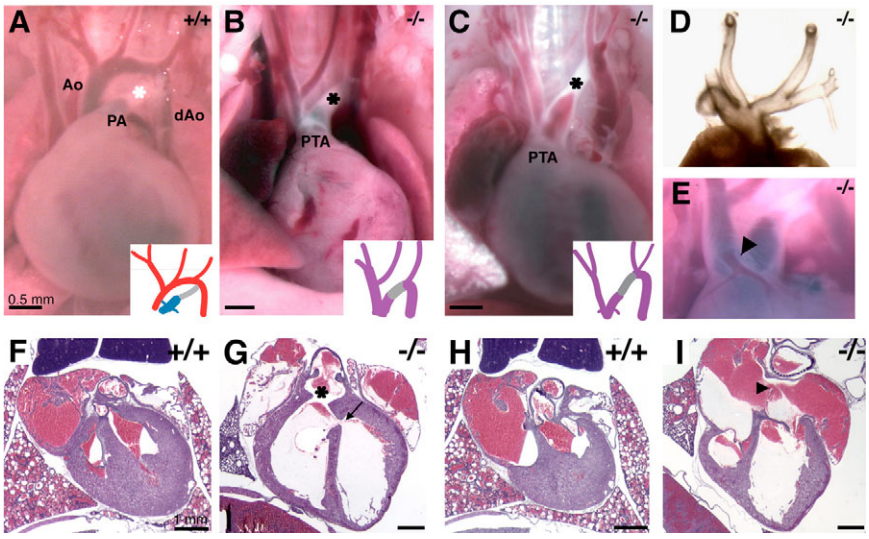

Fig. 2. Cardiovascular defects in *Ltbp1L*$^{-/-}$ mice. Gross dissections of newborn wild-type (**A**) and *Ltbp1L*$^{-/-}$ (**B-E**) mice with left or both atria removed to facilitate visualization of the great vessels. The ductus arteriosus is labeled with an asterisk in A-C. The great vessels are labeled as follows: Ao, aorta; PA, pulmonary artery; dAo, dorsal aorta; PTA, persistent truncus arteriosus. PTA with type B (B,E) and type C (C) IAA in *Ltbp1L* nulls. (D) PTA and a dextraposed aortic arch. (E) Ectopic position of a coronary artery (arrowhead). (**F-I**) Hematoxylin and Eosin-stained frontal sections of newborn hearts: (F,H) control; (G,I) mutant heart. PTA (G) is labeled with an asterisk. The membranous ventricular septum (G, arrow) and the atrial septum (I, arrowhead) are absent in the mutants.

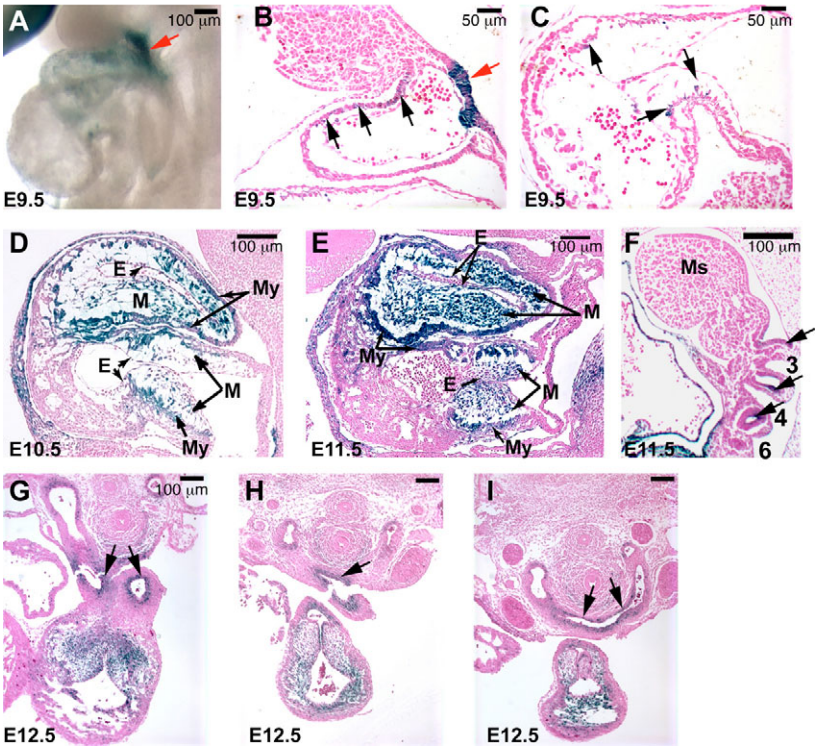

Fig. 3. *Ltbp1L* expression in the septating heart. Whole-mount (**A**) and lateral sections (**B**,**C**) of an E9.5 *Ltbp1L* heterozygous heart, stained with X-gal. Myocardial cells underlying outflow tract (OFT; B) and atrio-ventricular (AV; C) endocardial cushions express *Ltbp1L* (black arrows). Red arrows in A and B mark the thyroid primordium. (D-F) Lateral sections of E10.5 (**D**) and E11.5 (**E**,**F**) heterozygous hearts, stained with X-gal and Eosin. Myocardium (My) underlying OFT and AV cushions, mesenchymal cells (M) within the cushions and some E11.5 endocardial cells (E) express *Ltbp1L*. (F) Endoderm of pharyngeal pouches expresses *Ltbp1L* (arrows). The third, fourth and sixth pharyngeal arch arteries (PAAs) are labeled as 3, 4 and 6, respectively. (**G-I**) Transverse sections of an E12.5 heterozygous heart at the level of the ductus arteriosus (G), the fourth PAA (H) and the third PAA (I) stained with X-gal and Eosin. Arrows indicate *Ltbp1L*-expressing smooth muscle cells (SMCs) surrounding dorsal aortae and PAAs.

Pathological evaluation of newborn *Ltbp1L*$^{-/-}$ mice revealed cardiac OFT and aortic arch abnormalities (Fig. 2). Every *Ltbp1L* mutant exhibited defects in septation of the OFT resulting in a single outflow vessel exiting the heart (PTA) (Fig. 2B-E, asterisk in 2G). PTA results from failure of the truncus arteriosus, a vascular structure present in the developing embryo, to divide into the aorta and pulmonary artery.

In addition to PTA, most of *Ltbp1L* mutants displayed interruption of the aortic arch (IAA) (21/26). Normally, the aorta arises from the left ventricle, arches and descends as the dorsal aorta (Fig. 2A). In *Ltbp1L* nulls, the ascending aorta did not connect to the dorsal aorta. The only connection between the heart and dorsal aorta was the ductus arteriosus (Fig. 2A-C, asterisks). IAA in *Ltbp1L*$^{-/-}$ animals occurred either between the left common carotid and left subclavian arteries (type B) (Fig. 2B,E) or, rarely (1/21), between the brachiocephalic and left common carotid arteries (type C) (Fig. 2C). Some mutant hearts exhibited additional abnormalities, such as ectopic origin of a coronary artery, which arose from the mid-portion of the ascending aorta instead of the coronary sinus (Fig. 2E), or exhibited a right-sided aortic arch (4/26) (Fig. 2D).

Histological analysis of the mutant hearts revealed ventricular and atrial septum defects (vsd and asd, respectively) (vsd, arrow in Fig. 2G; asd, arrowhead in Fig. 2I). Ventricular communication is a mechanistic prerequisite for PTA, because the conotruncus must receive the blood from both ventricles. In all *Ltbp1L* mutants, the most basal portion of the ventricular septum, termed membranous septum, was missing (Fig. 2G).

Ltbp1L expression during OFT septation and remodeling of the associated vasculature

To understand the etiology of cardiac malformations in *Ltbp1L* mutants, we studied the expression of *Ltbp1L* at E9.5-E12.5, when crucial events in OFT septation and remodeling occur (Jiang et al., 2000). A promotorless *lacZ* cassette was inserted into the *Ltbp1L* locus during targeting, enabling us to follow reporter gene expression driven by the *Ltbp1L* promoter.

Ltbp1L expression in the heart was first detected in a few myocardial cells (Fig. 3A) underlying the OFT (Fig. 3B) and AV (Fig. 3C) cushions at E9.5 (Fig. 3A-C). As EMT advanced and CNCCs initiated invasion of the OFT, *Ltbp1L* expression broadened (Fig. 3D,E). At E11.5, *Ltbp1L* expression in the heart was at its highest: all of the myocardium underlying endocardial cushions (Fig. 3E, My), mesenchymal cells (Fig. 3E,M) and some endocardial cells (Fig. 3E,E) express *Ltbp1L* in the OFT and AV canal. Mesenchymal cells in the OFT at E11.5 (Fig. 3E, Fig. 4E,F) were of dual origin – endocardial and CNCCs – and they all expressed *Ltbp1L*. By contrast, pharyngeal mesenchyme, composed primarily of neural crest, did not express *Ltbp1L* (Fig. 3F, Ms; Fig. 4E,F, Ms). *Ltbp1L* expression in the pharynx was confined to the endoderm of pharyngeal pouches (Fig. 3F, arrows). We refer to CNCCs relocating from the dorsal neural tube to the OFT as 'migrating CNCC', whereas CNCCs in the OFT are defined as 'post-migratory'. The *Ltbp1L* expression pattern implies that post-migratory but not migrating CNCCs express *Ltbp1L*. *Ltbp1L* was also expressed by atrial myocardium and by cells surrounding dorsal aortae (SMCs) from E11.5 onwards [Fig. 4E,F, red arrowheads indicate SMCs surrounding dorsal aorta (dAo)]. However, at E12.5, *Ltbp1L* expression was detected in the subendothelial cells surrounding all PAAs and nascent pulmonary and aortic vessels (Fig. 3G-I, arrows indicate SMCs). *Ltbp1L* was also expressed by condensed mesenchymal cells in the OFT (Fig. 3G-I) and AV canal, myocardium of the right ventricle (in a patchy manner) and both atria (data not shown).

In summary, the *Ltbp1L* expression pattern within the E9.5-E12.5 window suggests possible Ltbp1L involvement in CNCC function and cardiac EMT.

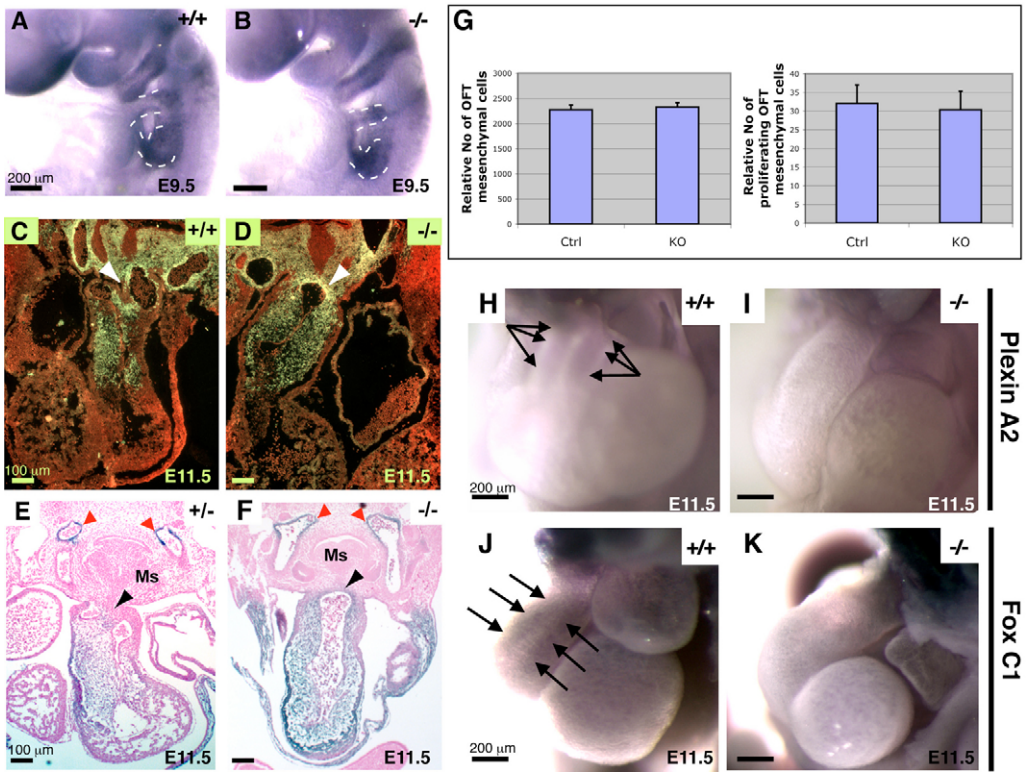

Fig. 4. The fate of CNCCs in *Ltbp1L* mutants. (**A**,**B**) Whole-mount in situ hybridizations of E9.5 wild-type (A) and knockout (KO; B) embryos, using a *Crabp1* ribo-probe. Broken lines outline streams of cardiac neural crest cells (CNCCs) migrating into the outflow tract (OFT). (**C**,**D**) Fate mapping of CNCCs in *Ltbp1L* mutants. E11.5 wild-type (C) and *Ltbp1L*$^{-/-}$ (D) transverse sections at the level at which the fourth pair of pharyngeal arch arteries (PAAs) branches out of the aortic sac. Green cells represent CNCCs. Arrowheads points to the aortico-pulmonary (AP) septum (C), or where it is missing (D). (**E**,**F**) Transverse sections of E11.5 heterozygous (E) and KO (F) embryos, stained with X-gal and Eosin. Blue cells express *Ltbp1L*. Black arrowheads indicate the AP septum (E) or its absence (F). Red arrowheads indicate *Ltbp1L*-expressing smooth muscle cells (SMCs) surrounding dorsal aortae. Ms, pharyngeal mesenchyme. (**G**) Quantification of mesenchymal cells and proliferating mesenchymal cells in E11.5 control and KO OFTs. Average of three sets of samples is shown. (**H-K**) Whole-mount in situ hybridization of E11.5 control (H,J) and KO (I,K) hearts using plexin A2 (H,I) and *FoxC1* (J,K) ribo-probes. Plexin A2 and *FoxC1* visualize post-migratory CNCCs in the control (arrows in H and J) but not *Ltbp1L*$^{-/-}$ OFT.

Cardiac neural crest function in *Ltbp1L* nulls

Failure in OFT septation has been attributed to defects in CNCC function (Creazzo et al., 1998). To determine whether lack of Ltbp1L affected CNCC functions, we analyzed the fate of migrating and post-migratory CNCCs visualized by virtue of their production of specific molecular markers.

First, we examined the distribution of Crabp1, a marker for migrating neural crest, by whole-mount in situ hybridization at E9.5 (Fig. 4A,B) and E10.5 (see Fig. S1I,J in the supplementary material). In *Ltbp1L*$^{-/-}$ embryos, migrating (Fig. 4A,B, broken lines) but not post-migratory (see Fig. S1I,J in the supplementary material, arrows) CNCCs expressed Crabp1 in a manner similar to that of wild-type embryos, suggesting normal migration of CNCCs into the OFT of *Ltbp1L*-null hearts.

We next examined the fate of cells of the CNC lineage permanently marked by yellow fluorescent protein (YFP) expression (Liu et al., 2006). The YFP-labeled CNCCs in E10.5 (data not shown) and E11.5 *Ltbp1L*$^{-/-}$ embryos migrated properly to pharyngeal arches, surrounded the PAAs and populated the endocardial cushions of the OFT in numbers comparable to controls (Fig. 4C,D, green cells). This result agreed with our histological analysis of control and mutant E10.5-E11.5 OFT endocardial cushions (Fig. 4E,F). The morphology and cellularity of mutant OFT endocardial cushions at E10.5 was indistinguishable from the controls (data not shown). However, although the cellularity of E11.5 OFT endocardial cushions in *Ltbp1L* mutants appeared normal, the morphology of the aortic sac was not. We observed normal onset of aortic sac septation in control embryos, marked by the formation of the AP septum (Fig. 4C,E, arrowheads). In mutant embryos, the AP septum was absent (Fig. 4D,F, arrowheads). Failure in AP septum formation and/or elongation was a consequence either of an insufficient number of CNCCs invading the OFT or a functional inadequacy of CNCCs residing in the OFT. The comparable cellularity of mutant and control OFT cushions indicated that the number of mutant CNCCs invading the OFT was normal. We quantified the number of mesenchymal cells in E11.5 OFTs in three pairs of age-matched control and mutant embryos to validate this assumption. Our quantification confirmed that mesenchymal cell number throughout the OFT endocardial cushions in control and mutant embryos was comparable (Fig. 4G, left). Furthermore, we determined the number of proliferating *Ltbp1L* mutant and control mesenchymal cells, stained by antibody to phospho-histone 3, in the E11.5 OFT. This analysis also yielded equivalent values for mutant and control embryos (Fig. 4G, right). The lack of the AP septum in *Ltbp1L*-null embryos could be a consequence of localized apoptosis of the forming AP septum rather than a failure of AP septum formation. Therefore, we stained transverse E11.0-E11.5 sections at the OFT level with antibody to

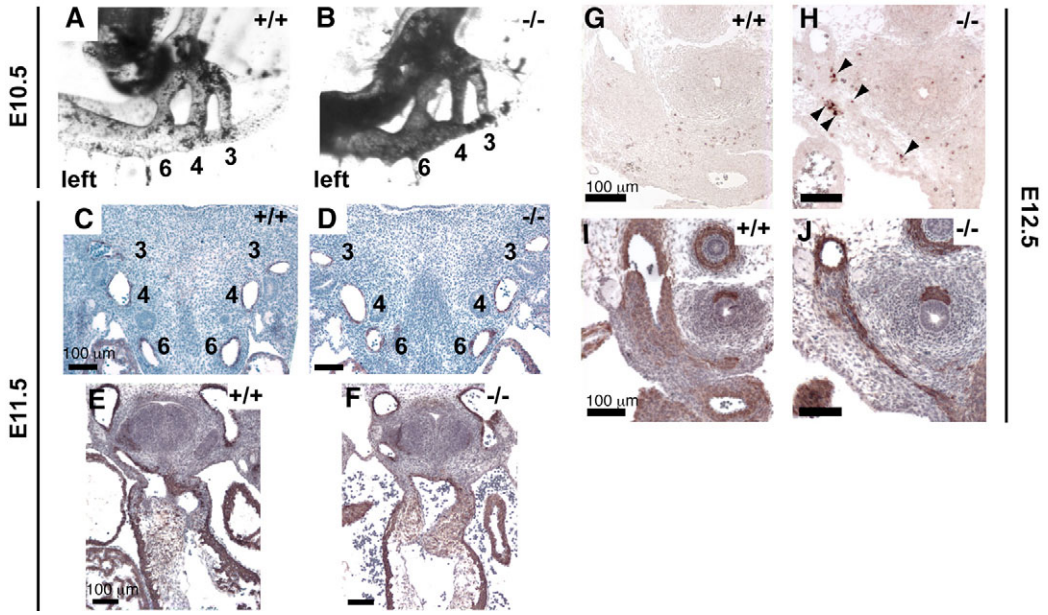

Fig. 5. Abnormal remodeling of PAAs in *Ltbp1L* mutants and normal differentiation of CNCCs into SMCs. (**A**,**B**) Visualization of pharyngeal arch arteries (PAAs) by India ink injection in E10.5 control (A) and knockout (KO; B) hearts. The third, fourth and sixth PAAs are properly formed in *Ltbp1L*$^{-/-}$ embryos. (**C**,**D**) Semi-transverse sections of E11.5 control and mutant embryos, stained with αSMA antibody and Hematoxylin. A ring of smooth muscle cells (SMCs; brown) surrounds all three pairs of PAAs both in control (C) and in KO (D) embryos. (**E**,**F**) Normal differentiation of CNCCs within the OFT of control and *Ltbp1L*$^{-/-}$ into SMCs. SMCs are visualized by staining with an antibody to αSMA. (**G-J**) Left fourth PAA is shown. Transverse sections of E12.5 control (G,I) and *Ltbp1L*$^{-/-}$ (H,J) embryos stained with active caspase 3 (G,H) or αSMA (I,J) antibody. Notice the clusters of apoptotic cells in the mutant left fourth PAA (arrowheads in H).

active caspase 3, which visualizes apoptotic cells. We observed no apoptosis in the KO OFT at the site of AP septum formation (data not shown). Thus, although the CNCCs migrated, invaded and proliferated normally within the OFT of *Ltbp1L* mutants, they did not form the AP septum, suggesting a functional defect of post-migratory CNCCs.

To investigate potential alterations in gene expression pattern of CNCCs in the OFT of *Ltbp1L* nulls, we analyzed the expression of two post-migratory CNCC markers, plexin A2 and FoxC1 (Gitler et al., 2004), in E10.5-E12.5 embryos by both whole-mount and slide in situ hybridization (Fig. 4H-K; see Fig. S1A-H in the supplementary material). Plexin A2 and *FoxC1* ribo-probes visualized two prongs of CNCCs in the OFT of control embryos (Fig. 4H,J, arrows; see Fig. S1A,C,E,G in the supplementary material). By contrast, very few mesenchymal cells in the *Ltbp1L* mutant OFT expressed plexin A2 or *FoxC1* (Fig. 4I,K; see Fig. S1B,D,F,H in the supplementary material). Our analyses consistently indicated that sufficient numbers of mesenchymal cells that were derived from neural crest populated the cushions. Intriguingly, *Ltbp1L*-mutant post-migratory CNCCs did not express two CNC molecular markers, plexin A2 and FoxC1, suggesting a defect in the post-migratory CNC gene expression pattern in mutant embryos.

Differentiation of *Ltbp1L*$^{-/-}$ CNCCs into SMCs is normal

Several studies have suggested an important role for TGF-β signaling in CNCC differentiation into SMCs (Chen and Lechleider, 2004; Wurdak et al., 2005). To investigate whether Ltbp1L deficiency might hamper CNCC differentiation into SMCs, we visualized SMCs surrounding the PAAs and within the OFT in E11.5-E12.5 tissue sections from mutant and control embryos by immunohistochemistry using an antibody against α-smooth muscle actin (αSMA; Acta2) (Fig. 5C-F,I,J). Despite the morphological abnormalities of the OFT and defective plexin A2 and *FoxC1* expression, the SMC specification of CNCCs in the OFT and surrounding vasculature in *Ltbp1L* mutants appeared normal.

Ltbp1L nulls display abnormal remodeling of PAAs

At E11.5, the third, fourth and sixth PAAs and dorsal aortae undergo a radical remodeling that ultimately results in an asymmetrical arterial system. Because *Ltbp1L*$^{-/-}$ mice develop IAA (type B, IAA-B), we examined the anatomy and patency of PAAs at E10.5-E11.5 using intracardiac India ink injections. Visualization of the third, fourth and sixth pairs of PAAs in 10.5-11.5 days post coitum (dpc) embryos showed no anatomical difference between the controls and mutants (Fig. 5A,B). Also, the αSMA staining of the mesenchyme surrounding the three pairs of PAAs showed normal recruitment of SMCs for the support of PAAs in *Ltbp1L*$^{-/-}$ embryos (Fig. 5C-F). However, soon after E11.5, the left fourth PAA regressed in mutant *Ltbp1L* embryos, causing the interruption of the aortic arch. The cause of this aberrant regression appeared to be enhanced apoptosis of the SMCs surrounding the left fourth PAA, as indicated by cleaved caspase-3 staining (Fig. 5G-J, arrowheads in 5H indicate apoptotic SMCs).

Decreased TGF-β signaling in the septating OFT of *Ltbp1L* nulls

Lack of canonical Tgf-β signaling in murine neural crest yields PTA associated with IAA-B (Choudhary et al., 2006; Wang et al., 2006; Wurdak et al., 2005). Given the similarity of cardiac defects in *Ltbp1L* nulls and *TgfbR1* and/or *TgfbR2* neural crest conditional

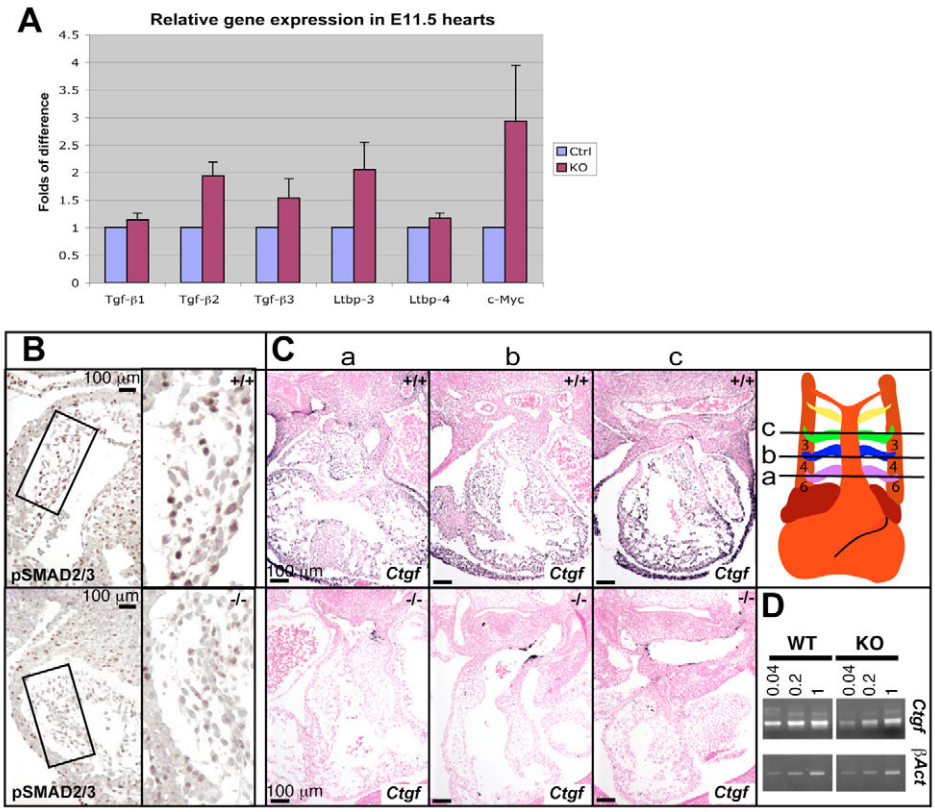

Fig. 6. Decreased Tgf-β signaling in the septating OFT of *Ltbp1L* mutants. (**A**) Quantification of Tgf-β1, Tgf-β2, Tgf-β3, Ltbp3, Ltbp4 and c-Myc expression by Q-RT-PCR, using cDNA isolated from three sets of E11.5 control (blue) and knockout (KO, burgundy) hearts. (**B**) Distribution of pSmad2 in E11.5 control (upper) and KO (lower) OFTs. Framed parts of the outflow tracts (OFTs) are magnified to show cardiac neural crest cell (CNCC)-specific attenuation of Smad2 phosphorylation. (**C**) *Ctgf* expression in E11.5 control and KO hearts estimated by in situ hybridization on sections taken at levels (a, b, c) indicated in the diagram and (**D**) semi-quantitative RT-PCR on cDNA isolated from E11.5 hearts.

mutants, and the fact that Ltbp1L interacts with all three isoforms of latent Tgf-β, we predicted that lack of Ltbp1L during murine development would result in decreased Tgf-β activity in the septating heart and associated vasculature.

First, we analyzed the expression of Tgf-β isoforms in E11.5 control and mutant hearts by Q-RT-PCR. The levels of Tgf-β1 expression in mutant and control hearts were comparable, whereas the expression of Tgf-β3 and especially Tgf-β2 was moderately and consistently increased in *Ltbp1L* nulls (Fig. 6A). Augmented Tgf-β2/β3 expression was reflected in increased Tgf-β2/β3 protein production (see Fig. S2 in the supplementary material). Interestingly, the expression of Ltbp3, which is the only chaperone of latent Tgf-β2 and Tgf-β3 besides Ltbp1, was augmented in *Ltbp1L* mutants. This suggests that Ltbp3 helps the secretion and ECM deposition of Tgf-β2 and Tgf-β3 in the absence of Ltbp1L.

We next examined Tgf-β activity in *Ltbp1L*$^{-/-}$ hearts during OFT septation by following the distribution of phosphorylated Smad2 (pSmad2) and the expression of two TGF-β early-response genes, connective tissue growth factor (*Ctgf*) and *c-Myc* (*Myc*).

Upon TGF-β binding to its receptor complex, Smad2 and/or Smad3 are phosphorylated and chaperoned to the nucleus by Smad4, where the pSmad2/3/4 complex influences the transcription of a myriad of genes. At E11.5, pSmad2 is localized in many myocardial, mesenchymal and endothelial nuclei of the control OFT (Fig. 6B). However, in the OFT of *Ltbp1L* nulls, pSmad2 is distributed in endothelial and myocardial but not mesenchymal nuclei (Fig. 6B), suggesting attenuation of Tgf-β signaling specifically in post-migratory CNCCs.

TGF-β increases *Ctgf* mRNA and protein synthesis in various cell types (Holmes et al., 2001; Moussad and Brigstock, 2000), whereas the expression of *c-Myc* is rapidly and profoundly down-regulated by TGF-β signaling (Warner et al., 1999). We followed the expression of *Ctgf* in E10.5-E12.5 embryos by in situ hybridization (E11.5 shown in Fig. 6C) and found a marked reduction in *Ctgf* mRNA synthesis in *Ltbp1L*$^{-/-}$ hearts, including in the mesenchymal cells of the OFT. This difference indicates a significant decrease of Tgf-β signaling in the developing hearts and pharyngeal apparatus of *Ltbp1L*-null embryos. Semi-quantitative RT-PCR analysis of RNA isolated from E11.5 mutant and control hearts confirmed reduced expression of *Ctgf* in *Ltbp1L*$^{-/-}$ versus control embryos (Fig. 6D). On the contrary, Q-RT-PCR analysis of *c-Myc* expression in E11.5 control and *Ltbp1L*$^{-/-}$ hearts showed a threefold increase in the *Ltbp1L*-null cDNA pool (Fig. 6A), again indicating a decrease in Tgf-β signaling.

Thus, although different Tgf-β isoforms are expressed at normal or moderately increased levels in developing *Ltbp1L*$^{-/-}$ hearts, the distribution of pSmad2 and expression of the Tgf-β response genes *Ctgf* and *c-Myc* in *Ltbp1L*$^{-/-}$ hearts suggest attenuation of Tgf-β signaling during the period crucial for OFT septation.

DISCUSSION

Mice with Ltbp1L deficiency display developmental abnormalities of the heart OFT, visualized as conotruncal, ventricular and atrial septation defects and abnormal remodeling of PAAs. These cardiac defects manifest as PTA and IAA, and are the underlying cause of post-natal lethality of *Ltbp1L* nulls. Failure in OFT septation and aberrant remodeling of PAAs in *Ltbp1L* nulls is a consequence of improper functioning of CNCCs. Ltbp1L is a component of the OFT and pharyngeal ECM during the time crucial for proper development of the great arteries and associated vessels. Because Ltbp1L covalently interacts with latent Tgf-β and directs its deposition into the ECM, we predicted that heart defects arising in the absence of Ltbp1L are due to aberrant Tgf-β activity. Indeed, we show decreased phosphorylation of a key Tgf-β signaling molecule,

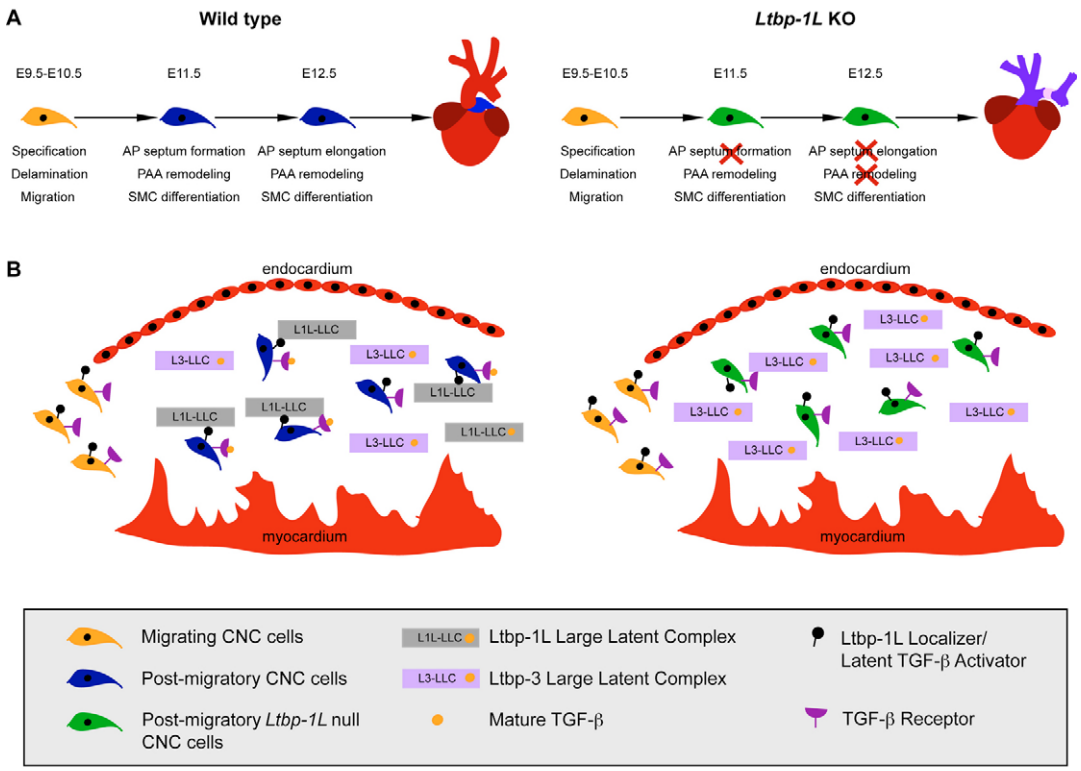

Fig. 7. Summary and a model for Ltbp1L requirement in the septating OFT. (**A**) Cardiac neural crest cells (CNCCs; orange) initially (E9.5-10.5) express genes necessary for proper specification, delamination and migration. As CNCCs relocate to the outflow tract (OFT) at E11.5, their gene expression program changes (blue CNCCs). This reprogramming correlates with morphological changes, such as aortico-pulmonary (AP) septum formation, remodeling of pharyngeal arch arteries (PAAs) and differentiation into smooth muscle cells (SMCs). At E12.5, CNCCs continue their gene expression program (blue cells) that enables them to elongate the AP septum, to continue remodeling PAAs and to differentiate into SMCs. *Ltbp1L*$^{-/-}$ CNCCs are normal and have a migratory trajectory undistinguishable from control littermates. The gene expression pattern characteristic for the migrating CNCCs also appears normal in *Ltbp1L*$^{-/-}$ embryos (orange CNCCs). However, when CNCCs invade the ECM in the OFT of *Ltbp1L* nulls, their gene expression program and function alters (E11.5, green CNCCs rather than blue) because they fail to form the AP septum. At E12.5, other morphological changes are evident – remodeling of defective PAAs and AP septum absence. However, CNCCs in *Ltbp1L* nulls successfully differentiate into SMCs. (**B**) Functional Tgf-β signaling is required for the maintenance of the appropriate gene expression program and function of post-migratory CNCCs. The ECM of the OFT contains both Ltbp1L-LLC and Ltbp3-LLC. Post-migratory CNCCs specifically recognize Ltbp1L-LLC and activate the latent Tgf-β. When the extracellular matrix (ECM) of the OFT is deprived of Ltbp1L, post-migratory CNCCs do not sufficiently propagate Tgf-β signals and, therefore, do not express genes required for their proper function (green CNCCs), resulting in persistent truncus arteriosus (PTA). Ltbp3 cannot substitute for Ltbp1L function, because post-migratory CNCCs do not recognize and act on Ltbp3-LLC.

Smad2, and altered expression of three Tgf-β-responsive genes – *FoxC1*, *Ctgf* and *c-Myc* – in *Ltbp1L*-null hearts, consistent with attenuated Tgf-β signaling. Post-migratory CNCCs in the OFT and surrounding the PAAs respond to decreased TGF-β activity by reprogramming their gene expression, which leads to CNCC malfunction. Indeed, post-migratory CNCCs unable to transmit TGF-β signals fail to septate the OFT and to properly remodel PAAs. We show that Ltbp1-L represents a crucial component of the ECM that regulates Tgf-β bioavailability during the development of great arteries and associated vasculature.

All Tgf-β isoforms are expressed in the developing heart, but disruption of Tgf-β genes in mice yields cardiac and great vessel abnormalities only in *Tgfb2*$^{-/-}$ mice (Sanford et al., 1997), in which the primary anomaly is a double-outlet right ventricle, associated with ventricular and atrial septum defects. Structural abnormalities of the aorta and its branches were detected with partial penetrance, whereas PTA was sporadic (1/24) (Bartram et al., 2001). By contrast, PTA associated with IAA is the consistent outcome of complete attenuation of Tgf-β signaling in mouse CNCCs (Choudhary et al., 2006; Wang et al., 2006; Wurdak et al., 2005). Complete penetrance of PTA in *Ltbp1L*$^{-/-}$ mice with a high incidence of IAA-B (81%) suggests a crucial role for Ltbp1L in Tgf-β presentation during the genesis of great vessels and their branches.

Mechanistically, PTA and IAA are two different conditions, but they often coincide with altered neural crest biology. The role of neural crest in PAA remodeling and OFT septation is obscure. PTA can arise from an insufficient number of CNCCs invading the OFT or a faulty function of the CNCCs that relocate to the OFT. Extensive analysis of CNCC fate in *Ltbp1L* mutants showed that CNCC specification, delamination and migration towards the cardiac tissue is normal. Also, CNCCs invade the OFT of *Ltbp1L* nulls in normal numbers, continue to divide properly within the OFT endocardial cushions and show no excessive apoptosis. However, *Ltbp1L*$^{-/-}$ CNCCs failed to septate the OFT. Choudhary et al. showed that Tgf-β represents a crucial cue for AP septum formation and that failure in AP septum formation results in PTA (Choudhary et al., 2006). Similarly, CNCCs in the OFT of *Ltbp1L* mutants did not properly regroup to form the AP protrusion, which ultimately hampered OFT septation. In addition, CNCCs that have relocated to the OFT of *Ltbp1L* mutants did not express *FoxC1* or plexin A2, markers of

proper CNCC function. FoxC1 is a member of the forkhead/winged-helix transcription factor family. Although post-migratory CNC and endothelial cells lining the endocardial cushions expressed FoxC1, its deficiency did not yield OFT septation defects. However, lack of *FoxC1* expression yielded improper PAA remodeling, resulting in interruption or coarctation of the aortic arch (Winnier et al., 1999). TGF-β upregulates *FOXC1* transcription in several human cancer cell lines and ectopic expression of *FOXC1* cDNA in HeLa cells, which lack both copies of the *FOXC1* allele, restores the potential of TGF-β1 to inhibit cell growth (Zhou et al., 2002). Therefore, *FOXC1* is a TGF-β-responsive gene, and failure of CNCCs in the OFT of *Ltbp1L* mutants to express *FoxC1* might be a consequence of decreased Tgf-β signaling. Plexin A2 is suggested to act as a co-receptor for semaphorin 3C (Sema3C) in its guidance of migratory CNCCs towards and within the cardiac OFT (Brown et al., 2001). The decreased number of plexin A2-expressing cells in E10.5-E12.5 OFTs of *Ltbp1L*$^{-/-}$ embryos is not attributable to a decreased number of post-migratory CNCCs, but it rather reflects plexin A2 downregulation, indicating that the role of plexin A2 in CNCC guidance within the OFT might be redundant. The role of Sema3C in CNCC guidance is highly dependent on the mouse strain; 129 and C57Bl/6 backgrounds (*Ltbp1L* mutants are of 129/C57Bl/6 background) have genes that can substitute for Sema3C in CNCC guidance (Brown et al., 2001).

Post-migratory CNCCs change their gene expression program in the absence of Ltbp1L. However, *Ltbp1L*$^{-/-}$ CNCCs maintain their ability to differentiate into SMCs supporting the outflow vessel and its branches, although the alteration of CNCC function resulted in PTA and IAA. Our results, and results of others (Choudhary et al., 2006; Wang et al., 2006), indicate that CNCC differentiation into SMCs might not be the only function of CNCC invasion of the OFT and pharynx. Indeed, the contribution of CNCCs to the valves of great arteries and SMCs supporting fetal and adult ascending aorta, the aortic arch and pulmonary trunk is moderate, considering the abundance of CNCCs during the septation of the OFT. Perhaps the major role of CNCCs in the OFT is that of an orchestrator of OFT septation, a process that relies on coordinated activities from the myocardium, endocardium and mesenchymal cells. Thus, the TGF-β pathway is crucial for the instructive role of CNCCs in the OFT.

PAAs in *Ltbp1L* mutants are properly formed and their remodeling unfolds normally until E12.5, when the left fourth PAA abruptly regresses. This regression is a result of the apoptosis of the SMCs surrounding the left fourth PAA. The same phenomenon has been described in mice with *TgfbR2* deficiency in the neural crest, and in some *Tgfb2* nulls (Choudhary et al., 2006; Molin et al., 2002). Apparently, proper Tgf-β signaling is crucial for correct remodeling of the fourth pair of PAAs. Initiation of *Ltbp1-L* expression in the subendothelial cells of PAAs at E12.5 coincides with the inappropriate regression of the left fourth PAA, suggesting that Ltbp1L is a crucial player in Tgf-β presentation to the CNCCs during PAA remodeling.

CNCCs first encountered Ltbp1L as they relocated to the OFT. Ltbp3, which binds all three latent Tgf-β isoforms, is also deposited in the OFT ECM (data not shown). The analysis of isoform-specific Tgf-β synthesis in *Ltbp1L*$^{-/-}$ hearts showed normal levels of Tgf-β1, but 2- and 1.5-fold increases in Tgf-β2 and Tgf-β3 synthesis, respectively. Augmented production of latent Tgf-β2 and Tgf-β3 was accompanied by a proportional increase in Ltbp3 synthesis, suggesting that the ECM of the mutant OFT contains sufficient amounts of latent Tgf-β. However, in spite of the fact that latent Tgf-β proteins are present in the heart ECM, the Tgf-β activity in *Ltbp1L*$^{-/-}$ septating hearts is reduced, as judged by pSmad2 staining and expression of the Tgf-β target genes *FoxC1*, *Ctgf* and *c-Myc*.

From the preceding data, we present the following summary (Fig. 7A) and propose a model (Fig. 7B) for Ltbp1L function in the septating OFT and branching vessels. CNCCs display a dynamic gene expression pattern as they delaminate, migrate and invade pharyngeal arches and heart. The migrating CNCCs transcribe a specific battery of genes (*Crabp1*, *FoxC1*, plexin A2, etc.). Cells with this gene expression pattern are depicted as orange in Fig. 7. At E11.5, CNCCs penetrate the ECM of the OFT and their gene expression program changes (Fig. 7, blue CNCCs), because they now cease expressing *Crabp-1*, continue transcribing plexin A2 and *FoxC1*, and start expressing other genes, including *Ltbp1L*, *Ctgf* and *αSma*. These changes correlate with the morphological changes, such as AP septum formation and SMC differentiation in the OFT, and PAA remodeling and SMC differentiation in the pharyngeal apparatus. At E12.5, CNCCs continue to express plexin A2, *FoxC1*, *Ctgf*, *Ltbp1L* and *αSma* (Fig. 7, blue CNCCs). As the AP septum elongates, PAA remodeling continues and CNCCs in the OFT and those surrounding the PAAs differentiate into SMCs. In *Ltbp1L* nulls, the trajectory and the gene expression pattern of migratory CNCCs is similar to that of the wild-type cells. However, as the mutant CNCCs invade the OFT, they attenuate the expression of certain genes, including *FoxC1*, plexin A2 and *Ctgf*, but continue to express *αSma*. This change in gene expression (illustrated by green rather than blue cells in Fig. 7) is accompanied by the lack of AP septum formation. By 12.5 dpc, the abnormal remodeling of the left fourth PAA is also apparent when the mutant and control embryos are compared. At that moment, it is not clear whether there are further differences in the CNCC gene expression profiles, but this is probably the case.

Fig. 7B depicts the proposed biochemical interactions of CNCCs with LLCs within the ECM of the OFT. In wild-type embryos, CNCCs interact with Ltbp1L-LLC and activate the latent Tgf-β. We propose that Tgf-β signaling is essential to maintain CNCC gene expression changes and that the delivery of active Tgf-β is dependent upon Tgf-β bound to Ltbp1L. The CNCCs must recognize and activate the latent Tgf-β specifically bound to Ltbp1L in the ECM, because Ltbp3-LLC cannot substitute for lost Ltbp1L-LLC. Therefore, CNCCs must display either a specific binding molecule for Ltbp1L or an activator of latent Tgf-β that requires Ltbp1L. The localizer/activator does not respond to LLC containing Ltbp3, perhaps, due to different ECM localization or sequence specificity in Ltbp1L recognition. In the absence of Ltbp1L, CNCCs are unable to generate active Tgf-β, resulting in the failure to effect proper gene expression and, ultimately, morphological changes. The model predicts specificity in terms of CNCC recognition and activation of Ltbp1L-LLC within the matrix. Characterization of this cell-matrix-interacting system is ongoing. We believe that identification of the molecules involved will enhance our understanding of the contribution of the ECM to the control of latent TGF-β activation.

We thank C. Colarossi for sharing her expertise in pathology; V. Kaartinen, USC, for cardiac ink injection training; and B. Dabovic, J. Munger and K. Yoshinaga, NYU SoM, for reading of the manuscript. This work was supported by NIH grants CA034282 and AR49698 to D.B.R. and NIH grant HL081336 and AHA Grant-in-Aid to D.E.G.

Supplementary material

Supplementary material for this article is available at http://dev.biologists.org/cgi/content/full/134/20/3723/DC1

References

Annes, J. P., Chen, Y., Munger, J. S. and Rifkin, D. B. (2004). Integrin alphaVbeta6-mediated activation of latent TGF-beta requires the latent TGF-beta binding protein-1. *J. Cell Biol.* **165**, 723-734.

Bartram, U., Molin, D. G., Wisse, L. J., Mohamad, A., Sanford, L. P., Doetschman, T., Speer, C. P., Poelmann, R. E. and Gittenberger-de Groot, A. C. (2001). Double-outlet right ventricle and overriding tricuspid valve reflect disturbances of looping, myocardialization, endocardial cushion differentiation, and apoptosis in TGF-beta(2)-knockout mice. *Circulation* **103**, 2745-2752.

Brown, C. B., Feiner, L., Lu, M. M., Li, J., Ma, X., Webber, A. L., Jia, L., Raper, J. A. and Epstein, J. A. (2001). PlexinA2 and semaphorin signaling during cardiac neural crest development. *Development* **128**, 3071-3080.

Chen, S. and Lechleider, R. J. (2004). Transforming growth factor-beta-induced differentiation of smooth muscle from a neural crest stem cell line. *Circ. Res.* **94**, 1195-1202.

Choudhary, B., Ito, Y., Makita, T., Sasaki, T., Chai, Y. and Sucov, H. M. (2006). Cardiovascular malformations with normal smooth muscle differentiation in neural crest-specific type II TGFbeta receptor (Tgfbr2) mutant mice. *Dev. Biol.* **289**, 420-429.

Creazzo, T. L., Godt, R. E., Leatherbury, L., Conway, S. J. and Kirby, M. L. (1998). Role of cardiac neural crest cells in cardiovascular development. *Annu. Rev. Physiol.* **60**, 267-286.

Dabovic, B., Chen, Y., Colarossi, C., Obata, H., Zambuto, L., Perle, M. A. and Rifkin, D. B. (2002). Bone abnormalities in latent TGF-[beta] binding protein (Ltbp)-3-null mice indicate a role for Ltbp-3 in modulating TGF-[beta] bioavailability. *J. Cell Biol.* **156**, 227-232.

Deckelbaum, R. A., Majithia, A., Booker, T., Henderson, J. E. and Loomis, C. A. (2006). The homeoprotein engrailed 1 has pleiotropic functions in calvarial intramembranous bone formation and remodeling. *Development* **133**, 63-74.

Flaumenhaft, R., Abe, M., Sato, Y., Miyazono, K., Harpel, J., Heldin, C. H. and Rifkin, D. B. (1993). Role of the latent TGF-beta binding protein in the activation of latent TGF-beta by co-cultures of endothelial and smooth muscle cells. *J. Cell Biol.* **120**, 995-1002.

Gitler, A. D., Lu, M. M. and Epstein, J. A. (2004). PlexinD1 and semaphorin signaling are required in endothelial cells for cardiovascular development. *Dev. Cell* **7**, 107-116.

Gomez-Duran, A., Mulero-Navarro, S., Chang, X. and Fernandez-Salguero, P. M. (2006). LTBP-1 blockade in dioxin receptor-null mouse embryo fibroblasts decreases TGF-beta activity: Role of extracellular proteases plasmin and elastase. *J. Cell. Biochem.* **97**, 380-392.

Gualandris, A., Annes, J. P., Arese, M., Noguera, I., Jurukovski, V. and Rifkin, D. B. (2000). The latent transforming growth factor-beta-binding protein-1 promotes in vitro differentiation of embryonic stem cells into endothelium. *Mol. Biol. Cell* **11**, 4295-4308.

Holmes, A., Abraham, D. J., Sa, S., Shiwen, X., Black, C. M. and Leask, A. (2001). CTGF and SMADs, maintenance of scleroderma phenotype is independent of SMAD signaling. *J. Biol. Chem.* **276**, 10594-10601.

Jiang, X., Rowitch, D. H., Soriano, P., McMahon, A. P. and Sucov, H. M. (2000). Fate of the mammalian cardiac neural crest. *Development* **127**, 1607-1616.

Kaartinen, V., Dudas, M., Nagy, A., Sridurongrit, S., Lu, M. M. and Epstein, J. A. (2004). Cardiac outflow tract defects in mice lacking ALK2 in neural crest cells. *Development* **131**, 3481-3490.

Kirby, M. L. and Waldo, K. L. (1995). Neural crest and cardiovascular patterning. *Circ. Res.* **77**, 211-215.

Koski, C., Saharinen, J. and Keski-Oja, J. (1999). Independent promoters regulate the expression of two amino terminally distinct forms of latent transforming growth factor-beta binding protein-1 (LTBP-1) in a cell type-specific manner. *J. Biol. Chem.* **274**, 32619-32630.

Liu, S., Liu, F., Schneider, A. E., St Amand, T., Epstein, J. A. and Gutstein, D. E. (2006). Distinct cardiac malformations caused by absence of connexin 43 in the neural crest and in the non-crest neural tube. *Development* **133**, 2063-2073.

Massague, J., Blain, S. W. and Lo, R. S. (2000). TGFbeta signaling in growth control, cancer, and heritable disorders. *Cell* **103**, 295-309.

Molin, D. G., DeRuiter, M. C., Wisse, L. J., Azhar, M., Doetschman, T., Poelmann, R. E. and Gittenberger-de Groot, A. C. (2002). Altered apoptosis pattern during pharyngeal arch artery remodelling is associated with aortic arch malformations in Tgfbeta2 knock-out mice. *Cardiovasc. Res.* **56**, 312-322.

Moussad, E. E. and Brigstock, D. R. (2000). Connective tissue growth factor: what's in a name? *Mol. Genet. Metab.* **71**, 276-292.

Muyrers, J. P., Zhang, Y., Testa, G. and Stewart, A. F. (1999). Rapid modification of bacterial artificial chromosomes by ET-recombination. *Nucleic Acids Res.* **27**, 1555-1557.

Nakajima, Y., Miyazono, K., Kato, M., Takase, M., Yamagishi, T. and Nakamura, H. (1997). Extracellular fibrillar structure of latent TGF beta binding protein-1: role in TGF beta-dependent endothelial-mesenchymal transformation during endocardial cushion tissue formation in mouse embryonic heart. *J. Cell Biol.* **136**, 193-204.

Noguera, I., Obata, H., Gualandris, A., Cowin, P. and Rifkin, D. B. (2003). Molecular cloning of the mouse Ltbp-1 gene reveals tissue specific expression of alternatively spliced forms. *Gene* **308**, 31-41.

Olofsson, A., Ichijo, H., Moren, A., ten Dijke, P., Miyazono, K. and Heldin, C. H. (1995). Efficient association of an amino-terminally extended form of human latent transforming growth factor-beta binding protein with the extracellular matrix. *J. Biol. Chem.* **270**, 31294-31297.

Sanford, L. P., Ormsby, I., Gittenberger-de Groot, A. C., Sariola, H., Friedman, R., Boivin, G. P., Cardell, E. L. and Doetschman, T. (1997). TGFbeta2 knockout mice have multiple developmental defects that are non-overlapping with other TGFbeta knockout phenotypes. *Development* **124**, 2659-2670.

Srinivas, S., Watanabe, T., Lin, C. S., William, C. M., Tanabe, Y., Jessell, T. M. and Costantini, F. (2001). Cre reporter strains produced by targeted insertion of EYFP and ECFP into the ROSA26 locus. *BMC Dev. Biol.* **1**, 4.

Sterner-Kock, A., Thorey, I. S., Koli, K., Wempe, F., Otte, J., Bangsow, T., Kuhlmeier, K., Kirchner, T., Jin, S., Keski-Oja, J. et al. (2002). Disruption of the gene encoding the latent transforming growth factor-beta binding protein 4 (LTBP-4) causes abnormal lung development, cardiomyopathy, and colorectal cancer. *Genes Dev.* **16**, 2264-2273.

Todorovic, V., Jurukovski, V., Chen, Y., Fontana, L., Dabovic, B. and Rifkin, D. B. (2005). Latent TGF-beta binding proteins. *Int. J. Biochem. Cell Biol.* **37**, 38-41.

Valenzuela, D. M., Murphy, A. J., Frendewey, D., Gale, N. W., Economides, A. N., Auerbach, W., Poueymirou, W. T., Adams, N. C., Rojas, J., Yasenchak, J. et al. (2003). High-throughput engineering of the mouse genome coupled with high-resolution expression analysis. *Nat. Biotechnol.* **21**, 652-659.

Wang, J., Nagy, A., Larsson, J., Dudas, M., Sucov, H. M. and Kaartinen, V. (2006). Defective ALK5 signaling in the neural crest leads to increased postmigratory neural crest cell apoptosis and severe outflow tract defects. *BMC Dev. Biol.* **6**, 51.

Warner, B. J., Blain, S. W., Seoane, J. and Massague, J. (1999). Myc downregulation by transforming growth factor beta required for activation of the p15(Ink4b) G(1) arrest pathway. *Mol. Cell. Biol.* **19**, 5913-5922.

Weiskirchen, R., Moser, M., Gunther, K., Weiskirchen, S. and Gressner, A. M. (2003). The murine latent transforming growth factor-beta binding protein (Ltbp-1) is alternatively spliced, and maps to a region syntenic to human chromosome 2p21-22. *Gene* **308**, 43-52.

Winnier, G. E., Kume, T., Deng, K., Rogers, R., Bundy, J., Raines, C., Walter, M. A., Hogan, B. L. and Conway, S. J. (1999). Roles for the winged helix transcription factors MF1 and MFH1 in cardiovascular development revealed by nonallelic noncomplementation of null alleles. *Dev. Biol.* **213**, 418-431.

Wurdak, H., Ittner, L. M., Lang, K. S., Leveen, P., Suter, U., Fischer, J. A., Karlsson, S., Born, W. and Sommer, L. (2005). Inactivation of TGFbeta signaling in neural crest stem cells leads to multiple defects reminiscent of DiGeorge syndrome. *Genes Dev.* **19**, 530-535.

Zhou, Y., Kato, H., Asanoma, K., Kondo, H., Arima, T., Kato, K., Matsuda, T. and Wake, N. (2002). Identification of FOXC1 as a TGF-beta1 responsive gene and its involvement in negative regulation of cell growth. *Genomics* **80**, 465-472.